

Application of overburden strength and deformation properties derived from drill cutting I_p data

Nils Kågeson Loe

BP EPTG, Chertsey Road, Sunbury-on-Thames Middlesex TW16 7LN (formerly Norsk Hydro, Bergen Norway)

Morten Gjetting Stage & Helle Foged Christensen

GEO, Maglebjergvej 1, DK-2800 Lyngby, Denmark

Ole Havmøller

Norsk Hydro, PB 7190, N-5020 Bergen, Norway

ABSTRACT:

Strength and deformation properties of clays are known to correlate with a standard geotechnical index parameter, the Plasticity Index, I_p , where these correlations are commonly used for characterising top soil or in the case of the offshore oil industry seabed analysis for foundations of offshore structures. By their nature, these studies are generally limited to the top 100+ m of the overburden. From a theoretical standpoint there is nothing to hinder the extension of such methods to greater depths other than the effects of diagenesis. This hypothesis is tested using drill cuttings from two North Sea fields of Tertiary age to characterise the overburden sequence. The results of the study are encouraging when compared with more conventional techniques using borehole log correlations suggesting that the plasticity index may offer a complimentary method for charactering overburden sequences for the purposes of borehole stability and reservoir compaction-seafloor subsidence.

1. INTRODUCTION

Direct determination of strength and deformation properties of overburden clay and shale by standard rock mechanics testing are time consuming. Furthermore, rock mechanics testing implies that the relevant formations are cored; unfortunately the coring process is expensive, often difficult to perform and may jeopardize the drilling operation. Nonetheless, knowledge of the strength and deformation of the overburden may be vital to the field development, e.g. well planning and wellbore stability, reservoir compaction and seafloor subsidence.

Drill cuttings are generally not used as a source for rock property evaluation partly because most laboratory techniques require pieces of core material larger than 5 mm which are of good to high quality and partly because, in many cases, drill cuttings are not preserved for further analysis once a lithological description has been completed. In those cases where drill cuttings are used the strength and stiffness properties are generally determined indirectly either from indentation or resonant acoustic wave techniques [1].

Strength and deformation properties of clays are known to correlate with a standard geotechnical index parameter, the Plasticity Index, I_p , where these correlations are commonly used for characterising top soil or in the case of the offshore

oil industry seabed analysis for foundations of offshore structures. By their nature, these studies are generally limited to the top 100+ m of the overburden. To date, there appears to be no documentation on the use of such correlations for evaluating the properties of 1000+ of overburden. Moreover, from a theoretical standpoint there is nothing to hinder the extension of such methods to greater depths other than the effects of diagenesis. In order to test this hypothesis, drill cuttings from two North Sea fields of relatively young geological age (lower Paleocene & younger) were used in a study to characterise the overburden sequence. The results of the study were compared with more conventional techniques using borehole log correlations.

2. GEOLOGICAL SETTING

Field 'A' is a deep water gas field situated 120 km west of the Norwegian coast (Kristiansund) and Field 'B', an offshore oil field, is situated 185 km west of Stavanger. In both fields, the overburden is Tertiary in age ranging from the Paleocene up to the Pliocene (figure 1). The burial depths appear to be substantially different in the two fields but this is primarily due to water depth: Field 'A' has a water depth of 800m whereas Field 'B' has a water depth of 150m. The actual overburden thickness in the two fields is similar: ca. 2000 m and 1600 m in

TERTIARY	Period	Group/Form.	m TVD	Field 'A'	m TVD	Field 'B'
				WD: 800		WD: 150
Pliocene	Nordland	Naust	1600	Soft, slightly calcareous silty claystone (more silty towards base)	925	Claystone with thin sand laminae
		Kai	1750	Upper sectn: mud/claystone Lower sectn: siliceous ooze/mudstone		
Miocene	Horstland	Brygge	2000	Ooze/mdst – silt sized, argillaceous, rel. soft & friable	1675	Soft to moderately firm claystone sequence with interbeds of silt, sand & carbonate cemented beds
Oligocene			OPAL-A/CT	2500		
Paleocene	Rogaland	Balder	2600	soft-/moderately form, slightly silty, tuffaceous mudstone	1685	soft-/moderately form, slightly silty, tuffaceous claystone
		Sele	2680	Moderately firm to hard slightly silty mudstone with occasional tuff & limestone	1695	Moderately firm to hard slightly silty claystone with occasional tuff & sandstone interbeds. Sandstone beds become more freq. near base of sequence.
		Lista	2880	Moderately firm to hard slightly silty mudstone with relatively frequent sand & calcareous interbeds	1735	Main reservoir sequence: turbidite sands fine to medium grained, poorly sorted, poorly consolidated.
		Våle /Heimdal				

Figure 1. Summary of overburden geology for Field 'A' and Field 'B'

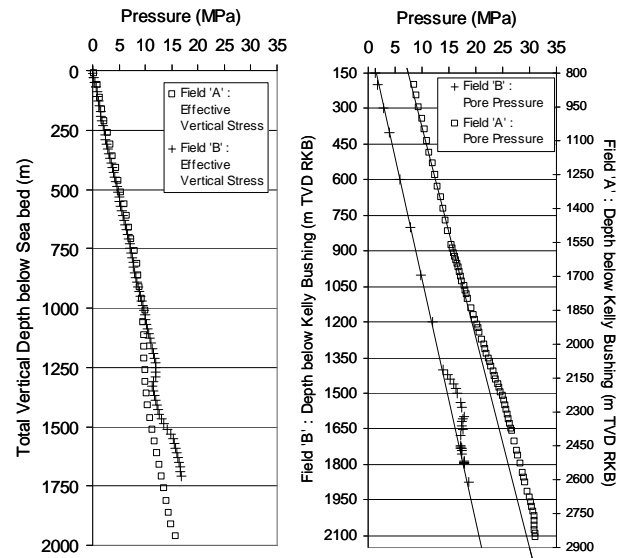


Figure 2. Effective Vertical stress and Pore pressure gradients in the overburden of Field 'A' and Field 'B'

Fields 'A' and 'B' respectively. This means that the effective vertical stress, i.e the net consolidation stress, in the two fields are comparable and only really differ where excess pore pressures occur (figure 2). In both cases, from drill cuttings, the overburden is described as a mixture of soft to stiff (consolidated) mudstones and sand layers. The mudstones in Field 'A' are dominated by pelagic-siliceous ooze sediments which are not present in Field 'B' (figure 1). The relatively young age of the overburden sequences and the fact that effective burial depths are less than 2000 m mean that the sediments have not experienced significant diagenesis; i.e. sediments have experienced mechanical compaction but very limited chemical compaction and lithification.

3. METHODOLOGY

The majority of fine grained (uncemented) sediments exist naturally in a 'plastic state'. The plasticity is due to the presence of clay minerals, very fine particles and organic material and is largely controlled by the water content of the sediment. The upper and lower limits of the range of water content over which the sediment exhibits plastic behaviour are known as the Atterberg limits and are defined as the 'liquid limit' (w_L) and the 'plastic limit' (w_P) [2]. The water content range is defined as the 'plasticity index' (I_P) where:

$$I_P = w_L - w_P \quad (1)$$

The I_P , w_L and w_P values can either be expressed as percentages or as decimal fractions. In the following calculations fractional values are used.

Since the 1940s a large number of studies have shown (empirically & semi-empirically) that for many clay rich and fine grained sediments the undrained compressive strength, compressibility, friction angle, in-situ stress ratio and consolidation ratio could be correlated with either the plasticity index or the plastic or liquid limits. These correlations are well documented in the geotechnical literature and a number of them are used here.

Prior to analysis the drill cuttings need to be pre-treated as they are nearly always contaminated with drilling mud. For water based drilling mud this contamination is in the form brine/salts, polymers and fine particles such as Barite or Calcium Carbonate – these particles are added to the drilling mud to increase density and assist in filtercake building. It was anticipated that the contamination of fine particles from the drilling mud would influence the plasticity index as they would reduce the relative clay content for a given volume thus reducing the material's plasticity. Furthermore, it was appreciated that the mud contamination would not be constant and would vary from sample to sample.

Measurement of the Atterberg limits on the drill cutting samples was in accordance with International testing standards [2]. In preparation, the drill cuttings were soaked/washed to remove the salts and polymers from the mud. During the soaking process the drill cuttings become disaggregated assisted by occasional mechanical agitation. The resulting slurry is passed through a no. 40 sieve in order to remove any large fragments and is then dried to approximately the liquid limit by evaporation and decanting of standing water. The liquid limit is then measured using the falling cone penetrometer method. The plastic limit is measured on an air-dried sub fraction of the drill cutting sample. Known quantities of distilled water are added to this sample until it takes on a putty like consistency and can be rolled into a ball. The plastic limit is then found by using the standard hand rolling technique. The reader should refer to either the ASTM testing standards or the general geotechnical literature for further details. The degree of barite and calcium carbonate contamination in the drill cutting samples is quantified using SEM-Microprobe analysis. A set of reference tests, which determine how the plasticity index varies with increasing amounts of barite or calcium carbonate content were used to correct the plasticity index measured on the contaminated drill cuttings (Appendix A). The corrected values were then used in further calculations of geotechnical properties.

In this study a number of correlations have been used to determine undrained compressive strength, stiffness, friction angle and in-situ stress ratio from plasticity index measurements on drill cuttings. The values obtained are compared with equivalent data calculated from borehole logs using more conventional techniques. The correlations used in this paper are summarized below

4. PLASTICITY INDEX CORRELATIONS

4.1. Undrained, unconfined compressive strength

Two of the more well known undrained strength correlations are used here:

Bjerrum & Simons (1960), [3]

$$\frac{UCS}{2 \cdot p'_o} = 0.45 \cdot (I_p)^{1/2} \quad (2)$$

Skempton & Henkel (1953), [4]

$$\frac{UCS}{2 \cdot p'_o} = 0.11 + 0.0037 \cdot I_p \quad (3)$$

where: p'_o – effective overburden stress (units in MPa)

It has been found that the above equations need an additional correction before they can be utilized. This is because the above equations are an approximation of the linear Mohr-Coulomb failure criteria and hence predict that shear strength increases linearly with depth (increasing p'_o). It is reasonable to suppose that for most argillaceous materials the failure criterion is non-linear, particularly at greater effective burial depths (500 m) due to the effects dewatering of the clay-silicate sheet structure has on friction angle. An additional, empirical correction is therefore made to equations 2 & 3 using a quadratic function of depth. The empirical correction is based on a best fit to UCS values measured on core plugs taken from the overburden.

$$UCS_{corr} = (1 - a_0 \cdot z^2 + a_1 \cdot z) \cdot UCS \quad (4)$$

where:

$$a_0 = 0.1167 \text{ (Field 'A')} \text{ \& } 0.1567 \text{ (Field 'B')}$$

$$a_1 = 0.1392 \text{ (Field 'A' \& 'B')}$$

4.2. In-situ Elastic moduli

From the geotechnical literature [5], the *in-situ* stress-strain modulus (equivalent to Young's modulus) for clays and silts is found to be proportional to the undrained strength (providing $I_p > 30\%$), where E (in units GPa) is given as:

$$E = (0.05 \text{ to } 0.25) \cdot UCS \quad (5)$$

The proportionality constant is determined by obtaining a best-fit to modulus values measured on core plugs. In the case of Field 'A' and Field 'B' the constant is found to lie between 0.095 to 0.13.

For the Poisson's ratio the following correlation is used (Worth 1975), [5]:

$$\nu \approx 0.25 + 0.00225 \cdot I_p \quad (6)$$

There are a significant number of published correlations for calculating in-situ bulk

compressibility from the plasticity index or liquid limit (e.g. [5]). Generally these expressions refer to the compressibility index either under virgin consolidation conditions (Compressibility Index, C_C) or under unloading-reloading (re-Compression Index, C_R) conditions – the latter also represent compressibility at current in-situ conditions. It may be argued that the re-compression index is most relevant for reservoir compaction-seafloor subsidence studies where, for example, the changes in effective stress in the overburden are relatively small and the overburden behaves elastically in response to the reservoir deformation. Equations 7 and 8 [5] show the re-compression index correlations used in this study:

$$C_R = 0.000463 w_L G_s \quad (7)$$

$$C_R = 0.00194 (I_p - 4.6) \quad (8)$$

The compressibility indices are terms not normally used in reservoir geomechanics so it is useful to convert these values to a more useable stress-strain modulus – the *constrained* modulus. This is done by using equation 9 below [5]:

$$M_R = \frac{(1 + w_N G_s) \sigma_v}{0.435 C_R} \quad (9)$$

where: w_N - in-situ (natural) water content;
 G_s - specific gravity of solids (= 2.65)

4.3. Effective Friction angle

A number of studies have investigated the relationship between the effective friction angle for normally consolidated clays and their plasticity. These studies generally show that friction angle decreases with increasing plasticity and that 80+% of the data fall within one standard deviation of a common trend where this trend can be defined as [6]:

$$\phi' = (60.6 \pm 4) \cdot (I_p)^{0.24} \quad (10)$$

where: ± 4 - denotes the standard deviation from the common trend.

The effective friction angle can also be independently determined from the effective stress ratio (K_0) as is described in the following section. The friction angle can be combined with cohesion (c), derived from the UCS, in a simple Mohr-

Coulomb failure criterion which can be then implemented in basic borehole stability models:

$$c = \frac{UCS \cdot (1 - \sin \phi')}{2 \cdot \cos \phi'} \quad (11)$$

4.4. In-situ stress ratio; K_0

The ratio of effective horizontal (σ'_h) to vertical effective stress (σ'_v) is expressed by a factor called the 'coefficient of lateral effective stress' or 'lateral effective stress ratio'. Of particular interest is the special case for no lateral deformation, termed the 'lateral stress ratio at rest' (K_0), as this represents conditions in a passive sedimentary basin. Hendron, Brooker & Ireland (1965), and cited in [5, 6] defined the relationship between K_0 , consolidation ratio (CR) and plasticity index which is now commonly used in geotechnic design. For a consolidation ratio of between 1 and 4 (normally to lightly overconsolidated sediment) the relationship can be defined in the following way [6]:

$$K_0 = [\ln(I_p)^{0.1537} \cdot \ln(CR)^{0.334} + 1] + \ln(CR)^{0.10558} + 0.0841 \quad (12)$$

where: CR - consolidation ratio which describes the compaction history of the sediment; normal consolidation =1, overconsolidation > 1, underconsolidation < 1; and where [6, 7]:

$$K_0 = \frac{\sigma'_h}{\sigma'_v} \approx (1 - \sin \phi') \quad (13)$$

The above relationships can be used to indicate how the effective stress ratio varies with depth through the overburden and, knowing the effective vertical stress (effective overburden stress), calculate the effective horizontal stress. From equation 12 it can be seen that the effective stress ratio is logarithmically proportional to the plasticity index (and the consolidation ratio). This means that mudstone intervals with high plasticity will have a larger effective stress ratio and lower friction angle - this is a common observation for dense clay and mudstone sequences [3, 5, 6, 7 & 8].

5. LOG BASED CORRELATIONS

It is possible from a range of different borehole logs to derive various rock mechanic properties using either empirical or theoretical relationships. A combination of open-hole and cased-hole sonic

velocity logs, together with Gamma-ray and Density logs are available for the overburden in field 'A' and 'B'. Using these logs, rock strength and stiffness trends have been derived from the relationships given in the following sections.

5.1. Unconfined compressive strength, UCS

The UCS of the overburden has been determined using two empirical techniques which utilise the P-wave sonic log (DTCO) and Gamma-ray log respectively. The two log types are respectively linked to the porosity and clay content of the formation and so are a good basis for compressive strength calculations.

The UCS is calculated from the P-wave sonic log using the following relationship where this is a modified form of the correlation established for shale-type materials by Horsrud *et al* [9]. The modification is made to give a best-fit UCS values measured on core plugs taken from the overburden.

$$UCS = 1.184 \times 10^6 \cdot DTCO^{-2.5} \quad (14)$$

where: UCS is in units of MPa and DTCO units of $\mu\text{s}/\text{ft}$.

An alternative technique is to derive the compressive strength from the Gamma-ray (γ -ray) log. This is generally a much more simplistic scaling approach and takes the form of:

$$UCS = \gamma\text{-ray} / 20 \quad (15)$$

where the scaling factor of 20 is determined from a best-fit to measured values on core data; UCS in units of MPa.

5.2. In-situ Elastic moduli

From Hooke's law, the Young's Modulus and Poisson's ratio can be derived from the P- and S-wave sonic velocities in the following way:

$$E = 2(1 + \nu) \cdot \rho \cdot V_s^2 \quad (16)$$

$$\nu = \frac{V_p^2 - 2 \cdot V_s^2}{2(V_p^2 - V_s^2)} \quad (17)$$

where: E is in units of GPa; V_p and V_s in units of m/s and ρ in units of Kg/cc.

Also from Hooke's law, the Constrained Modulus, M can be derived from the Poisson's ratio and Young's modulus:

$$M = \frac{(1 - \nu) \cdot E}{(1 + \nu)(1 - 2\nu)} \quad (18)$$

Caution is necessary when using equation 16, 17 and 18 as they are derived assuming isotropic linear elasticity to which few natural materials truly conform.

5.3. Effective Friction angle

The P-wave velocity has been correlated to the the friction angle in shale sequences by Lal [10]. The proposed relationship is given as follows:

$$\phi' = \frac{V_p - 1000}{V_p + 1000} \quad (19)$$

where: V_p in units of m/s.

5.4. In-situ stress ratio; K_0

From elasticity theory the effective stress ratio, K_0 can be related to the Poisson's ratio by the following well known expression:

$$K_0 = \nu / (1 - \nu) \quad (20)$$

The Poisson's ratio can be either derived from the sonic logs, equation 17 or from drill cuttings, equation 6.

6. VALIDITY OF PLASTICITY INDEX & LOG CORRELATIONS FOR CHARACTERISING THE OVERBURDEN

It should be remembered that the objective of this paper is to test the hypothesis that the standard geotechnical plasticity index (I_p) (Atterberg Limits) can be employed to characterize the strength and stiffness of the overburden. As such, the validity of the method is tested against established borehole log correlations based mostly on the sonic and density logs. Only a qualitative comparison is therefore possible as it is not necessarily true that the borehole log based calculations are the more accurate or the more correct. Where core measurements of strength and stiffness are available

then both the log based and drill cutting based methods have been adjusted/calibrated so neither method is truly independent. If the drill cuttings based methods give comparable results to the log based correlations then it can be argued that the former can lend an additional, supportive role to the latter for characterizing the overburden.

Figures 2 and 3 present the combined results of the drill cutting and log based analysis – included are the input data; i.e. the plasticity index (I_p) and the sonic and density logs. The gamma-ray log is not shown due to the lack of space.

6.1. *Input parameters – general comments*

In terms of the input data, the density logs for both fields ('A' and 'B') show a gradual density increase with depth which is consistent with increasing consolidation. The sonic logs show a similar trend – here the sonic slowness decreases with depth reflecting the increased sonic velocity due to increased density. The S-wave slowness is more sensitive to changes in lithology and demonstrates a step profile where there is continuous data coverage (sporadic data for Field 'A' due to problems with the logging tool).

The plasticity index (I_p), as defined by the liquid limit and plastic limit also increases with depth. The plastic limit is defined as the difference between the liquid and plastic limit values when expressed in percentage terms (eqn 1). For both field 'A' and 'B' the liquid limit is relatively constant with depth - about 75% (occasionally $\pm 15\%$) where this is an overall reflection of the uniformity of the clay mineralogy and grain size. In contrast the plastic limit gradually decreases with depth reflecting the increasing consolidation and this therefore results in an increase in plasticity index with depth.

The main exception to the uniformly increasing density, sonic velocities and plasticity index (I_p) trends with depth is observed in Field 'A' between 1600 and 2000 mTVD. It is at the lower end of this depth interval that the Opal A-Opal CT transition occurs and with it a change in the consolidation of the siliceous ooze. As described earlier, the ooze appears softer and more friable above the transition boundary where this appears to be reflected in the plasticity index and log responses. Other variations in the general depth trends occur but these can be correlated with subtle changes in lithology.

6.2. *Unconfined Compressive Strength (UCS)*

The UCS is derived from the plasticity index measured on drill cuttings using equations 2 and 3 and from the sonic log and gamma-ray log using equations 14 and 15 respectively.

There is generally good agreement (± 1 MPa) between the sonic, gamma-ray and drill cutting (plasticity index) based strength correlations down to depths of 2300 mTVD and 1650 mTVD for Fields 'A' and 'B' respectively (figures 2 & 3). There is also generally good agreement between the log-based and drill cutting-based methods and direct strength measurements on core plugs (some deviations occur and these are discussed later). The overriding trend is one of gradual strength increase (4 to 6 MPa) with increasing depth. Below these depths, the gamma-ray and drill cutting strength correlations remain in agreement but the sonic log-derived rock strength shows a relatively marked strength increase. A precise reason for this deviation is not known but may either reflect:

- i. a subtle diagenetic effect such as the initial occurrence of intergranular cement - the gamma-ray and plasticity index based methods are insensitive to cementation as they are primarily triggered by clay content and mineralogy;
- ii. a change in the pore pressure gradient in the overburden adjacent to the reservoir. In both Field 'A' and 'B' there is a weak overpressure trend in the overburden but the reservoirs themselves have near hydrostatic pressure (figure 2). The reduction in pore pressure immediately above the reservoir will increase the effective stress and thus the sonic velocity as well as the degree of consolidation – leading to apparent (eqn 14 not normalized to pore pressure) and real increases in strength respectively.

Measurements on core samples taken from Field 'A' below 2300 mTVD are in agreement with both the sonic log and gamma-ray/drill cutting trends: strength measurements made on samples of stiff-dense mudstones agree with the sonic log strength trend whereas measurements made on weak claystones agree with the gamma-ray/drill cutting trend (figure 2). Given this, it is difficult to conclude which of the strength trends are more correct.

In Field 'A' an anomaly is observed in the drill cutting/plasticity index strength data in the depth interval 2250 to 2350 mTVD (figure 2). The drill cutting based data shows a sudden strength increase in this interval relative to the sonic and gamma-ray trends. There is no clear correlation with lithology (no variation indicated in well site or later reports) but the event may be related to a local variation in clay mineralogy or clay properties (e.g. activity) that affect the plasticity. The SEM-micro probe analysis indicates some variation in relative volumes of clay forming elements but there is no consistency and the data set is too small to say whether or not the increase in strength and stiffness is real.

Another anomalous event observed in the Field 'A' well data occurs in the depth interval 2550 to 2600 mTVD. The gamma-ray based strength profile deviates from the common trends in this interval and show a marked reduction in strength. The event is linked to the presence of volcanic ash, which affects the gamma-ray signal.

In Field B, a similar anomalous event is observed in the depth interval 1665 to 1675 mTVD (figure 3). Three strength measurements on core plugs were taken in this interval and of these, two show much higher strengths than that predicted by either of the borehole log-based correlations or by the drill cutting/plasticity index correlations. The core sample from this interval is described as "highly" heterogeneous containing repeated thin layers of hard (cemented) mudstone, soft-reactive (occasionally fractured) mudstone and volcanic ash. The stronger layers dominate the core plug measurements simply because of the ease of sampling. The volcanic ash layers have influenced the gamma-ray signal causing a dip in the strength trend based on this log. The drill cutting based strength trend shows neither high or low strength values and may be a result of an averaging effect as the drill cuttings are sampled every 10 m.

Finally, it should be noted that equations 2 and 3 provide two methods for calculating strength from drill cuttings. Over the range of plasticity indices measured on the drill cuttings the two equations produce two closely spaced parallel trends. It is not possible say which of these equations is more correct and it would be fair to say that the relative difference in derived strength values (0.3 to 0.5 MPa) is probably within the uncertainty range of the overall method. It is therefore suggested that

either or both equations can be used with equal validity.

6.3. *Young's Modulus*

The Young's modulus is derived from the plasticity index measured on drill cuttings and from the sonic logs using equations 5 and 16 respectively.

In Field 'A', in the depth interval 1550 to 2000 mTVD, there is remarkably good agreement in the sonic log derived Young's modulus, the plasticity index/drill cutting derived Young's modulus and direct measurements on core plugs (figure 2). Between 2000 and 2850 mTVD the correlation is less certain as the S-wave data is incomplete resulting in large gaps in the sonic log derived Young's modulus trend. Where there is data it appears to be in agreement with the drill cutting derived data. The latter indicates a relatively uniform, gently increasing, Young's modulus trend with depth – ranging from 0.25 GPa at 1550 mTVD to 0.5 GPa at 2000 mTVD. Below 2000 mTVD, there is a sharp increase in the sonic log derived Young's modulus that is consistent with the available core plug measurements in addition to the sonic log based rock strength (UCS). If drill cutting data were available for 2000+ mTVD it would be unlikely to correlate with this sonic log based data given the fact that the drill cutting based Young's modulus is simply a linear correlation with rock strength (eqn 5). It was noted earlier that the rock strength trends diverge at around 2000 mTVD – see previous section. .

In Field 'B' the agreement between the sonic log based Young's modulus and the plasticity index/drill cutting based Young's modulus appears less clear (figure 3). Above 1650 mTVD, Young's modulus derived from the plasticity index is consistently 0.5 GPa greater than that calculated from the sonic log (note: a better correlation can of course be derived by adjusting the constant used in equation 5 but of interest here is the overall robustness of the method rather than exact agreement). Below 1650mTVD there is good agreement between the Young's Modulus derived from the sonic log and drill cuttings and that measured on core plugs. The drill cuttings based data does not pick-out the peaks observed in the sonic log based Young's modulus but as suggested earlier, for rock strength, this may be a result of an averaging effect as the drill cuttings are sampled every 10 m.

6.4. Poisson's ratio

The Poisson's ratio is derived from sonic logs using equation 17 and from the plasticity index measured on drill cuttings using equation 6.

A very consistent difference is observed in the Poisson's ratio values derived from the drill cutting's plasticity index and sonic logs. For both Field 'A' and 'B' the Poisson's ratio determined from drill cuttings varies between 0.3 and 0.35 whereas the sonic log derivation indicates a Poisson's ratio value in the range 0.45 to 0.35. Furthermore, slightly conflicting depth trends are observed - the sonic log based data indicates that Poisson's ratio decreases slightly with depth but in contrast, the drill cutting based data suggest a relatively constant value (possibly slightly increasing trend) with depth. It should be noted that the depth trends are weak relative to the difference in overall magnitude. There are no measurements on core plugs from the overburden with which to make a judgment on which method is the more correct. Where core measurements exist, in the reservoir, they are in agreement with the sonic log based trend but there is no comparable drill cutting data.

The difference in the derived values may well lie in the origins of the correlations used. Equation 6, relating Poisson's ratio to plasticity index, is empirically derived from laboratory data whereas equation 17, the sonic log correlation, is based on elasticity theory. Linked to this is the fact that the sonic log is measured in-situ and may include either a poro-elastic component (due to the slight overpressure in the overburden) or a weak tectonic component - or both. Such factors cannot be accounted for in the simple laboratory empirical approach. Either way, the difference in the derived Poisson's ratio values can result in an approximate difference of 10% if used to calculate the horizontal stress from the vertical stress using a uniaxial strain model.

6.5. Constrained Modulus

The Constrained Modulus is derived from the plasticity index using equations 7 to 9 and from the sonic logs using equations 16 to 18. The latter method is an extension of elasticity theory and the former represent a pair of empirical correlations based on laboratory data - equation 8 uses the plasticity index (I_p) and equation 7 the liquid limit (w_L). There are no direct measurements of constrained modulus (bulk compressibility) on

overburden core with which to compare so it is not known which method gives a more correct value. It is therefore encouraging to see some agreement between the two calculation methods as seen in figures 2 & 3.

In Field 'A', in the depth interval 1550 to 2000 mTVD, the sonic log derived Constrained Modulus appears to agree reasonably well with that derived from the liquid limit (w_L) using equation 7. In contrast, the Constrained Modulus determined from the plasticity index using equation 8 shows much greater variations in modulus values with depth and therefore do not correlate well - it should be noted that the large gaps in the sonic log data necessarily restrict the comparison. Below 2000 mTVD, the sonic log based Constrained Modulus shows a marked increase corresponding to the stiffening observed in the Young's modulus data and is a result of a sonic velocity increase at reservoir depth (see earlier discussions on Young's modulus).

In Field 'B', in the depth interval 1450 to 1650 mTVD, there is some agreement between the sonic log derived Constrained modulus and that derived from the liquid limit (eqn 7) as well as the plasticity index (eqn 8). Modulus values determined from equation 7 appear to form a lower bound to the data trend whereas values calculated from equation 8 seem to coincide with and exhibit a similar sinuous trend to the sonic log based data. An exact comparison is not possible due to a lack of data points but weak correlation is nonetheless present. Below 1650 mTVD, the sonic log based trend deviates from the drill cuttings based trends where this is again a reflection of the increasing Young's modulus and sonic velocities within and immediately above the reservoir.

Of the drill cutting based methods, and given the limitations of the data set, the Constrained Modulus values derived from the liquid limit measured on drill cuttings appears to correspond best with the sonic log derived values. This argument is partly supported by observations from the geotechnical literature where it is reported that compressibility values determined from a clay soils liquid limit correspond best with values measured from laboratory tests (and some field scale plate load tests), [3, 4, 5, 6 & 7].

6.6. Friction angle

The friction angle is derived from the sonic logs using equation 19 and from the plasticity index measured on drill cuttings using equation 10. Both

methods are empirical and based on experimental databases of varying size and quality – the database for the drill cutting correlation is probably the larger and more reliable [6 & 10].

A consistent difference is observed in the friction angle derived respectively from the plasticity index measured on drill cuttings and the sonic log. Values determined from the latter correlation are always lower than those derived from the former. Furthermore, in the case of Field ‘A’ the depth trends determined from the two correlations are conflicting – the sonic log based friction values shows an increase in friction with depth whereas the plasticity index based friction decreases with depth. For Field ‘B’ the contrast is less clear-cut. Here again, the sonic log based correlation shows a marked increase in friction with depth but the drill cutting based data suggests a relatively constant friction angle with depth

As no measurements of friction angle on overburden core material are available from Fields ‘A’ and ‘B’ it is not possible at the present time to say whether the drill cutting based or the sonic log based correlations is the more reliable. From general reporting in the geotechnical literature, it is usual for the friction angle to decrease with depth for uncemented clay rich sediments as with increasing consolidation the clay platelets (particles) become aligned and macro laminations and fissuring develop – the net effect of which is to reduce the friction angle. In contrast, if the sediment becomes cemented then the friction angle can be expected to increase. It was stated at the beginning of this paper that the overburden sequences in Fields ‘A’ and ‘B’ have experienced mechanical compaction but very limited chemical compaction and lithification due to their relatively young geological age and the fact that effective burial depths (total vertical depth less water depth) are less than 1800 m. This set of statements would therefore suggest that the friction angle derived from the plasticity index is more reliable than that determined from the sonic log although it should be pointed out that this argument is somewhat tenuous without corroborating data from laboratory measurements.

6.7. *In-situ stress ratio, K_0*

The K_0 ratio is derived from the plasticity index using equation 12 and from the sonic logs using equation 20. The latter method is an extension of elasticity theory and the former is an empirical

correlation based on an extensive laboratory data set [5, 6].

In Field ‘B’, at the top of the depth interval investigated (1450 mTVD), the K_0 ratio determined from the sonic log is greater than that calculated from the plasticity index. The difference in the derived values decreases with depth as a result of converging trend lines – both methods predict that K_0 decreases with depth where the sonic log derived data shows the greatest reduction. The two K_0 trends appear to coincide and show similar amplitude variations below 1600 mTVD.

In Field ‘A’ the comparison is less certain due to the large gaps in the sonic log data. From initially giving similar values at the top of the depth interval investigated (1550 mTVD) the K_0 values determined from the sonic log and plasticity index diverge where the former predict higher values. That said, the overall depth trend in the interval 1550 to 2050 mTVD is quite similar. Both data sets show an initial reduction in K_0 down to a depth of 1700 mTVD but below this the K_0 ratio is predicted to increase again. Below 2050 mTVD the lack of sonic log data makes any comparison meaningless so none is attempted. The K_0 ratio calculated from the drill cuttings suggests a weak increase with depth below 2050 mTVD where this is consistent with the observed decrease in friction angle with depth (see previous section & eqns 12 & 13).

There are no direct measurements of the K_0 ratio on overburden core from Fields ‘A’ and ‘B’ so it is not known which of the two correlations - sonic log correlation or the plasticity index correlation – is the more correct. Also, as discussed previously for the Poisson’s ratio the sonic log is measured in-situ and may therefore include either a poro-elastic or a weak tectonic component which will affect both the calculated Poisson’s ratio and K_0 ratio. Such factors will not be accounted for in the empirical plasticity index correlation and may be one reason why the two methods do not necessarily agree.

7. CONCLUSION

A set of correlations for determining the strength and deformation properties of clays from a standard geotechnical index parameter, the Plasticity Index, I_p , have been applied to drill cuttings taken from 2 North Sea fields. The objective of the exercise has been to test whether such correlations are valid for characterising an overburden sequence of 1000+ m. The validity of the results has been tested against

published correlations, theoretical and empirical, for determining strength and stiffness from borehole logs.

For compressive strength (UCS) and Young's modulus good agreement is found between the plasticity index derived values and those determined from the borehole logs (sonic & gamma-ray). The mutual correlation is further supported by available laboratory measurements on core plugs taken from the overburden sequences.

For Poisson's ratio, Constrained Modulus, friction angle and in-situ stress ratio, K_0 , less satisfactory agreement between the plasticity index and borehole log derived values are observed. With respect to Poisson's ratio and K_0 , one possible explanation for the discrepancy is that the borehole logs are measured in-situ and may contain a hidden poro-elastic or tectonic component which can not be accounted for or quantified when using the empirical (laboratory derived) plasticity index correlations. Generally however, these four parameters have not been measured in the laboratory on relevant overburden core so it is not certain which of the correlations, borehole log vs. plasticity index, gives the more correct values.

The results from the comparative analysis suggest that the plasticity index, and its associated correlations, offers a valid method for characterising the overburden particularly where borehole log data is absent (as demonstrated by Field 'A' data). It should be noted however, that the technique is restricted to relatively young geological sequences that have not been subjected to significant diagenesis – in particular chemical diagenesis and lithification. The advantage of the plasticity index method is that it is simple to perform and can be easily adapted for rig-site analysis.

Further work is required to test the applicability and robustness of the plasticity index technique but the results to date are encouraging.

8. ACKNOWLEDGEMENTS

The authors would like to acknowledge Norsk Hydro Oil & Gas for generously supporting the R&D work presented here and permitting its publication.

REFERENCES

1. Nes O.M, Horsrud,P., Sønstedt E.F., Holt R.M, Ese A.M, Økland, D. & Kjørholt H.(1996). Rig-site and laboratory use of CWT acoustic velocity measurements on cuttings. SPE 50982.
2. ASTM D4318-00. Standard test method for Liquid Limit, Plastic Limit and Plasticity Index of soils.
3. Bjerrum, L. and Simons, N.E. (1960). Comparison of shear strength characteristics of normally consolidated clays. *1st PSC, ASCE*, pp 711-726
4. Skempton A.W. and Henkel, D.J. (1953). The post-glacial clays of the Thames estuary at Tilbury and Shellhaven. *3rd ICSMFE*, vol. 1., pp 302-308
5. Bowles J.E. (1996). *Foundation Analysis and Design* (5th ed). McGrawHill.
6. Lambe T.W. & Whitman R.V. (1979). *Soil Mechanics*. John Wiley & Sons.
7. Schofield, A.N. and Wroth, C.P., 1968. On the generalised stress-strain behaviour of "wet" clay. *Eng. Plasticity*, Cambridge University Press, pp. 525-609
8. Roscoe, K.K and Schofield, A.N. (1963). Mechanical behaviour of an idealised "wet" clay. *2nd ECSMFE*, Wiesbaden, 1, pp. 47-54
9. Horsrud P. (2001) Estimating Mechanical Properties of Shale From Empirical Correlations. SPE 56017
10. Lal,M (1999). "Shale Stability: Drilling Fluid Interaction and Shale Strength", SPE 54356, presented at the 6th SPE LAPEC Conference, Caracas, Venezuela.

APPENDIX A

The expressions given below are used to correct the measured plasticity index for the contamination of fine particles from the drilling mud. The relative volume of the contaminant is determined using SEM-Microprobe.

Correction for Barite contamination:

$$\Delta IP = .0.0138 \%B . 0.021 \quad (A1)$$

ΔIP is the change in Plasticity Index (%)

$\%B$ is the volume percentage of Barite.

Correction for Calcium carbonate contamination:

$$\Delta I_p = - 3 \cdot 10^{-4} c_{Calcite} - 8 \cdot 10^{-4} c_{Calcite} + 0.0014 \quad (A2)$$

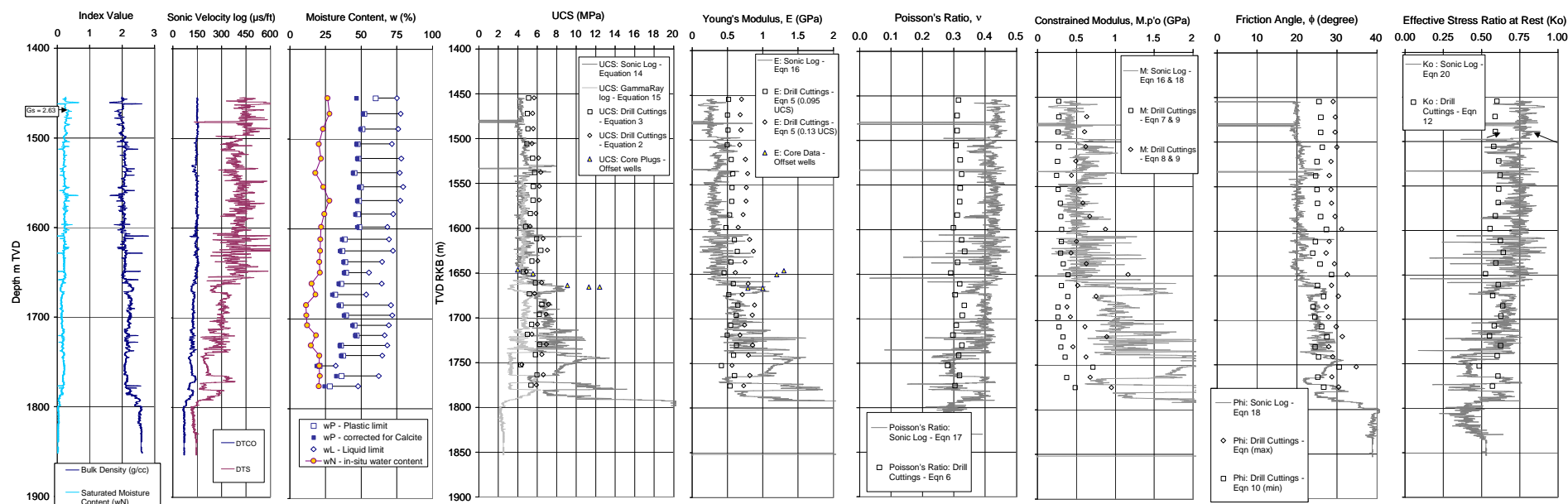


Figure 3 Characterization of Overburden in Field 'B' using Drill Cutting and Bore Hole Log data

Data is plotted with respect to total vertical depth beneath Kelly bushing (TVD RKB). Log based data is indicated by continuous line profiles whereas drill cutting based data is indicated by open symbols. Drill cutting measurements are derived from wet drill cutting samples collected every 5 to 10m.

Input data - going from left, the first three depth-logs show the input data used in the analysis:

i) Density log (& derived in-situ water content log); ii) Sonic logs – P-wave (DTCO) and S-wave (DTS) ;

iii) Log of plasticity index parameters: Liquid limit (w_L) - open diamonds; Plastic limit (w_P) – open squares; in-situ (saturated moisture) content of the drill cuttings as measured in the laboratory – coloured circles. The Plasticity Index (I_p) is the difference between the liquid limit and the plastic limit and is indicated by the horizontal bar joining the open diamonds and squares. The Plasticity Index of the drill cuttings is corrected for Barite contamination and the magnitude of this correction is shown by adjusting the values for the Plastic limit. The adjusted values are shown by the solid blue squares. The corrected Plasticity Index is used in subsequent calculations.

Output data – Rock parameters calculated from borehole logs (sonic log – dark grey line; gamma-ray log – light grey line) and Plasticity Index data from Drill cuttings (open squares/diamonds) - going from left to right:

iv) Unconfined Compressive Strength (UCS); v) Young's Modulus (E); vi) Poisson's ratio (ν) vii) Constrained Modulus (M); viii) Friction angle (ϕ); ix) In-situ stress ratio (K_0)